Journal of Thermal Analysis and Calorimetry, Vol. 92 (2008) 2, 513–522

ISOTHERMAL KINETICS OF PHOTOPOLYMERIZATION AND THERMAL POLYMERIZATION OF *bis*-GMA/TEGDMA RESINS

J. M. Morancho[*], *A. Cadenato, X. Fernández-Francos, J. M. Salla and X. Ramis*

Laboratori de Termodinàmica, Departament de Màquines i Motors Tèrmics, ETSEIB, Universitat Politècnica de Catalunya
Diagonal 647, 08028 Barcelona, Spain

The purpose of this work is to analyse certain kinetic features related to thermoinduced and photoinduced isothermal curing in the 25/75 mass% *bis*-GMA/TEGDMA system. The kinetic parameters associated with photo and thermal curing were determined and compared using an isoconversional procedure and the kinetic model was obtained by means of a reduced master plot. In photocuring, the kinetic results obtained by means of this phenomenological methodology were compared with those obtained on the basis of mechanistic considerations. In this case, we estimated the propagation and termination constants associated with photocuring at different conversions. When the phenomenological procedure is performed, the rate constant decreases slightly during the curing process and the autoacceleration effect of the process is demonstrated in the kinetic model, which is autocatalytic. However, in the mechanistic model, this same effect is noted through an increase in the rate constants, while it is assumed that the kinetic model is in the order of n with n=1.

Keywords: *dimethacrylate monomers, isothermal kinetics, photocuring, thermal curing*

Introduction

In this paper, we examine the thermoinduced and photoinduced free radical copolymerization of mixtures of dimethacrylate monomers containing 2,2-*bis*[4-(2-hydroxy-3-methacryloyloxypropoxy) phenyl]propane (*bis*-GMA) and triethyleneglycol dimethacrylate (TEGDMA) in proportions of 75/25 mass% (*bis*-GMA/TEGDMA). It may be reasonable assumed that these systems constitute simplified models of the resins used at present in commercial filling composites, veneers, etc. [1, 2]. After inducement by heat or UV radiation, the dimethacrylate monomers form three dimensional thermostable structures. These networks are formed by the free radical cross-linking of the C=C double bonds in the terminal methacrylate groups of the polymers used [3, 4]. The polymerization of multifunctional monomers, particularly when UV-induced, is often anomalous, especially in relation to curing kinetics. This behaviour includes autoacceleration and autodeceleration, incomplete conversion of all functional groups, a delay in volume shrinkage with respect to equilibrium and unequal reactivity of the double bonds of the dimethacrylate monomers [1, 5–7]. The following are some of the factors that may influence this behaviour: physical impediments (viscosity of the resins and vitrification) that may reduce the mobility of the monomers, concentration of free radical species, formation of microgels, temperature, concentration of the initiator, incident radiation, diffusion and solubility of oxygen, etc.

The initiation step is a determining factor in the free radical systems and can condition the final properties of the material. When the process is thermoinduced, the activation energy, E, associated with this step is directly considered to be that of the thermal decomposition of the initiator, while with photoinducement, E is considered to be very small and takes a value of zero [8, 9]. This value for E implies that the rate of photopolymerization is much higher than that of thermal polymerization as autoacceleration is far more prominent and the system may not occupy the equilibrium volume, since the volume shrinkage rate is much lower than the chemical reaction rate [10].

The most characteristic aspect of the polymerization of multifunctional monomers is autoacceleration, which is followed, after a maximum value for the curing rate is attained, by deceleration that leads to very low rates during the final part of the reaction. This phenomenon, which is analogous to what occurs in autocatalytic reactions, means that we can assume the polymerization of dimethacrylate monomers to be an autocatalytic process, in contrast with the n^{th} order reactions that predict the maximum rate of polymerization at zero conversion. As a rule, autocatalytic effects are related to the formation of an intermediate species that sharply accelerates the reaction. In the case of the polymerization of multivinyl compounds, this effect is normally related to the reduction of the termination reactions, which are due to limitations on the diffusion of reactive chain ends. Thus, the in-

---

[*] Author for correspondence: morancho@mmt.upc.edu

1388–6150/$20.00

Akadémiai Kiadó, Budapest, Hungary
Springer, Dordrecht, The Netherlands

creased concentration of free radicals gives rise to high rates of polymerization [7].

The kinetics of the curing of dimethacrylate monomers can be studied using two different methodologies: phenomenological [7, 11, 12] or mechanistic [8, 10, 12–16].

The phenomenological method applied to curing normally uses the n^{th}-order and autocatalytic reaction models.

In the n^{th}-order model, it is assumed that the reaction occurs according to the following equation:

$$\frac{d\alpha}{dt}=k(1-\alpha)^n \qquad (1)$$

where $d\alpha/dt$ is the reaction rate, k is the rate constant that depends on temperature, α is conversion after a time t and n is the order of the reaction.

In the autocatalytic model (so-called pseudo-autocatalytic), the effect of autocatalysis is manifest in an independent order of reaction, m, called the autocatalytic exponent:

$$\frac{d\alpha}{dt}=k\alpha^m(1-\alpha)^n \qquad (2)$$

The curing of dimethacrylate monomers is normally dealt with using this latter model, due to its autocatalytic effect.

Most kinetic studies of the mechanistic type are based upon a known kinetic equation that expresses the proportionality between the polymerization rate and the concentration of monomers and free radicals in an exponent equal to one [12, 17–19]. This is the same as assuming an n^{th}-order kinetic model in which n=1.

In this paper we compare the isothermal kinetics of thermocuring and photocuring of dimethacrylate monomers using the phenomenological method. We used this methodology in a previous paper [20] to study the dynamic curing of these same systems; it consists in determining the activation energy and a second kinetic parameter (which includes the model and a pre-exponential factor) by means of an isoconversional method. The model and the pre-exponential factor are separated once the model has been established by means of the reduced master curves [21]. This procedure is a fast and accurate alternative for determining k, n and m by means of multilinear regression for each curing temperature and does not require pre-establishing the model or any other kinetic parameter [7, 22, 23].

Another aim of our work was to compare the phenomenological and mechanistic methodologies with the isothermal photocuring of dimethacrylate monomers. As has already been mentioned, these two methodologies are based on different sets of assumptions and, therefore, lead to different results. The phenomenological method only requires a series of isothermal tests at constant illumination and the kinetic model used, as a rule, is of the autocatalytic type. The mechanistic methodology used [14] requires a combination of steady-state tests at constant illumination and non-steady-state tests performed with no illumination. In addition, the 1^{st}-order kinetic model must be used and calculations can only be made over a short range of conversions. As a rule, both procedures give similar activation energies, since these energies are independent of the fixed kinetic model, while the rate constants show opposing trends. When the phenomenological methodology is used with a 1^{st}-order kinetic model, the results are similar to those obtained using the mechanistic approach, although the methodology is much simpler and the results can be obtained over the full range of conversions.

Experimental

Materials

Bis-GMA (M_w=512) and TEGDMA (M_w=286) monomers supplied by Aldrich were used as received. A dispersion of benzoyl peroxide in dibutyl phthalate with a content of 40 mass% (Luperox AFR40, Aldrich) was used as a thermal initiator. The photoinitiator used was 2,2-dimethoxy-2-phenyl-acetophenone supplied by Aldrich.

Samples were prepared by dissolving the initiator in the TEGDMA monomer by means of magnetic stirring for 2 h at 30°C. *Bis*-GMA was subsequently added to obtain a formulation with a *bis*-GMA concentration of 25 mass%. It was stirred for 2 h at 30°C and kept at –20°C before use to prevent polymerization. In the case of thermal curing, mixtures containing 2 phr of initiator (2 parts per 100 parts of mixture, *w*/*w*) were used, whilst those used for photocuring contained 3 phr of initiator.

Methods

DSC calorimetry

Calorimetric analyses were carried out using a Mettler DSC-821^e calorimeter with a TSO801RO robotic arm. Samples of approximately 5 mg in mass were cured in aluminium pans in a nitrogen atmosphere.

Non-isothermal experiments using benzoyl peroxide as initiator were performed between 0 and 250°C at heating rates of 5, 7.5, 10 and 15°C min^{-1} in order to determine the total reaction heat. A value of 345 J g^{-1} was taken as the total reaction heat, calculated as the average value for heat reaction obtained non-isothermally at the different heating rates, since the FTIR analysis of the cross-linked material did not show any residual double bonds.

Isothermal experiments using benzoyl peroxide as the initiator were performed at temperatures of 90, 93, 96 and 100°C.

The isothermal photopolymerization study by means of photo-DSC was performed at different temperatures (20, 30, 40, 50, 60, 70, 80, 90, 100, 120°C) using a Mettler DSC-821^e calorimeter. It was modified to make irradiation possible using a Hamamatsu Lightningcure LC5 (Hg–Xe lamp) with two beams, one for the sample side and the other for the reference side. Two scans were performed on each sample in order to subtract the thermal effect of the UV irradiation on the sample from the photocuring experiment. Each scan consisted of 4 min of temperature conditioning, 10 min of irradiation and finally 4 more min without UV light. A similar procedure was used for the dark reaction, but the light was turned off at different times when the material reached different degrees of curing. The incident light intensity at the sample pan position was measured as 12.8 mW cm^{-2} (by the carbon black method).

The absolute degree of conversion at a time *t* was calculated as the quotient between the heat released up to *t* and the total reaction heat associated with complete conversion of all reactive groups. The reaction rate, dα/d*t*, was expressed as the ratio between the instant heat released (d*h*/d*t*, calorimetric signal) and the total heat of the reaction. In order to compare the phenomenological and mechanistic procedures, we used the absolute degree of conversion for kinetic analysis, and only used the relative degree of conversion to determine the kinetic model using the reduced master curves [24]. The relative degree of conversion at a time *t* was calculated as the quotient between the heat released up to *t* and the total heat generated in an isothermal experiment.

Phenomenological kinetic analysis

If we accept the Arrhenius equation, the kinetics of the reaction is usually described by the rate equation:

$$\frac{\mathrm{d}\alpha}{\mathrm{d}t}=kf(\alpha)=Af(\alpha)\exp\left(-\frac{E}{RT}\right) \tag{3}$$

where *t* is time, *A* is the pre-exponential factor, *E* is the activation energy, *T* is the absolute temperature, *R* is the gas constant and *f*(α) is the differential conversion function.

Isoconversional methods

In general, the phenomenological kinetic analysis was carried out using an isoconversional method. The basic assumption of these methods is that the reaction rate at constant conversion is only a function of the temperature [25].

By integrating the rate equation, Eq. (3), in isothermal conditions we obtain:

$$\ln t=\ln\left[\frac{g(\alpha)}{A}\right]+\frac{E}{RT} \tag{4}$$

where *g*(α) is the integral conversion function [20]. According to integral Eq. (4), the activation energy and the constant ln[*g*(α)/*A*] can be obtained for a constant value of α from the slope and the intercept of the linear relationship ln*t* *vs*. T^{-1}, respectively. Once *g*(α) is determined, we can calculate *A* for each conversion.

As an alternative, by applying logarithms to Eq. (3), the differential isoconversional method suggested by Friedman [26] is obtained:

$$\ln\left(\frac{\mathrm{d}\alpha}{\mathrm{d}t}\right)=\ln[Af(\alpha)]-\frac{E}{RT} \tag{5}$$

The linear plot of ln(dα/d*t*) *vs*. T^{-1} obtained from DSC thermograms recorded at several heating rates makes it possible to determine *E* and the kinetic parameter ln[*Af*(α)] for every value of α. Once *f*(α) is determined, we can calculate *A* for each conversion.

To compare the kinetics of thermoinduced curing with those of photoinduced curing, we used the integral isoconversional method (Eq. (4)) [20, 27]. The comparison of the phenomenological and mechanistic methodologies with UV-induced curing was made by means of differential methods (Eq. (5)), since in mechanistic terms, all the kinetic equations are used in their differential forms.

Integral and differential master plots

Using α=0.5 as reference point, the following differential master equation is easily derived from Eq. (3):

$$\frac{f(\alpha)}{f(0.5)}=\frac{\mathrm{d}\alpha/\mathrm{d}t}{(\mathrm{d}\alpha/\mathrm{d}t)_{0.5}} \tag{6}$$

where $(\mathrm{d}\alpha/\mathrm{d}t)_{0.5}$ and *f*(0.5) are the reaction rate and the differential conversion function at α=0.5, respectively. An expression that is equivalent to Eq. (6) can be used on the basis of an integral method. Recently, some authors [21, 28] have applied a universal expression to the master plots using the concept of generalised time introduced by Ozawa [29].

In order to determine the kinetic model, different conversion functions were studied: diffusion (D_1, D_2, D_3 and D_4), Avrami–Erofeev ($A_{3/2}$, A_2, A_3 and A_4), power law (P_2), phase-boundary-controlled reaction (R_2 and R_3), reaction-order *n* (*n*=3, 2, 1.5 and 1) and autocatalytic (*n*+*m*=1, 2 and 3 with different values of *n* and *m*) [20, 21].

Mechanistic kinetic analysis

The kinetic study using a mechanistic method was carried out following the approach used by Tryson and Shultz [14]. In the experiments using light, the rate of disappearance of the monomer (–d[*M*]/d*t*) (which is proportional to the calorimetric signal) can be written as:

$$-\frac{\mathrm{d}[M]}{\mathrm{d}t}=k_\mathrm{p}\left(\frac{\Phi I_\mathrm{abs}}{k_\mathrm{t}}\right)^{1/2}[M] \tag{7}$$

where k_p and k_t are the rates of propagation and termination, respectively, and the formation of free radicals is the result of the product of the quantum yields and the photon absorption rate ΦI_abs. This equation can be deduced based on the following hypotheses: a) the reaction rate of any free radical with a monomer does not depend on the type of radical; b) the termination reactions are bimolecular; c) transfer reactions are disregarded; d) there is a steady-state concentration of free radicals; e) due to theoretical considerations, it is assumed that the rate depends on the first power of monomer concentration.

For the purpose of comparing the phenomenological and mechanistic methodologies, Eq. (7) can be expressed depending on the degree of conversion as:

$$\frac{\mathrm{d}\alpha}{\mathrm{d}t}=k_\mathrm{p}\left(\frac{\Phi I_\mathrm{abs}}{k_\mathrm{t}}\right)^{1/2}(1-\alpha) \tag{8}$$

Replacing the rate constants with the Arrhenius equation in Eq. (8) and taking logarithms, we can write:

$$\ln\frac{\mathrm{d}\alpha}{\mathrm{d}t}=\ln\left[A_\mathrm{p}\left(\frac{\Phi I_\mathrm{abs}}{A_\mathrm{t}}\right)^{1/2}\right]+\ln(1-\alpha)-\frac{E_\mathrm{p}-E_\mathrm{t}/2}{RT} \tag{9}$$

Comparing Eqs (8) and (9) with Eqs (3) and (5) for a 1st-order kinetic model, the apparent global activation parameters (*A*, *E*, *k*) as determined phenomenologically are related to the parameters determined mechanistically (A_p, A_t, E_p, E_t, k_p, k_t) by means of the following expressions:

$$\ln A=\ln\left[A_\mathrm{p}\left(\frac{\Phi I_\mathrm{abs}}{A_\mathrm{t}}\right)^{1/2}\right];\quad E=E_\mathrm{p}-E_\mathrm{t}/2;\quad \ln k=\ln\left[k_\mathrm{p}\left(\frac{\Phi I_\mathrm{abs}}{k_\mathrm{t}}\right)^{1/2}\right] \tag{10}$$

Determination of rate constants

If we rewrite the expressions for the rate of disappearance of the monomer (Eqs (7) and (8)) we obtain:

$$\frac{k_\mathrm{p}}{k_\mathrm{t}^{1/2}}=\frac{-\mathrm{d}[M]/\mathrm{d}t}{(\Phi I_\mathrm{abs})^{1/2}[M]}=\frac{\mathrm{d}\alpha/\mathrm{d}t}{(\Phi I_\mathrm{abs})^{1/2}(1-\alpha)} \tag{11}$$

The ratio $k_\mathrm{p}/k_\mathrm{t}^{1/2}$ can be calculated empirically on the basis of DSC data at different temperatures under constant lighting conditions by means of Eq. (11). For the system studied, we assumed a value of 0.6 for the quantum yield Φ. I_abs, the rate of photon absorption ($1.15\cdot10^{-3}$ mol s^{-1} L^{-1}), was calculated as explained in [30].

By turning off the light during a DSC experiment, we obtain:

$$\frac{[M]}{(-\mathrm{d}[M]/\mathrm{d}t)}=\frac{k_\mathrm{t}}{k_\mathrm{p}}t_\mathrm{dark}+\frac{[M]_0}{(-\mathrm{d}[M]/\mathrm{d}t)_0} \tag{12}$$

the ratio $k_\mathrm{t}/k_\mathrm{p}$ can be calculated, at different conversions, on the basis of the slope of the representation of [*M*]/(–d[*M*]/d*t*) *vs.* the dark reaction time (t_dark), for samples that have been partially light-cured.

Equation (12) can also be expressed on the basis of the degree of conversion as:

$$\frac{(1-\alpha)}{(\mathrm{d}\alpha/\mathrm{d}t)}=\frac{k_\mathrm{t}}{k_\mathrm{p}}t_\mathrm{dark}+\frac{(1-\alpha)_0}{(\mathrm{d}\alpha/\mathrm{d}t)_0} \tag{13}$$

In both expressions, the subscript zero indicates $t_\mathrm{dark}=0$ (time when light was turned off).

To deduce Eqs (12) and/or Eq. (13), we assumed the following hypotheses: a) when the light is turned off, the production of free radicals is zero (non-steady-state conditions); b) kinetic constants remain invariable throughout the test without light; c) changes in the concentration of the monomer are negligible during the dark reaction.

On the basis of the values of $k_\mathrm{p}/k_\mathrm{t}^{1/2}$ (from steady-state data, constant illumination, Eq. (11)) and $k_\mathrm{t}/k_\mathrm{p}$ (from non-steady-state rate, dark reaction, Eqs (12) or (13)), obtained experimentally by DSC, we can determine the individual values of k_p and k_t.

Results and discussion

Figures 1 and 2 show the DSC thermograms for the thermoinduced and UV-induced isothermal curing, respectively. It can be observed that photocuring occurs at a much faster rate at the same temperature. This same effect is found in curing times. Thermal curing shows a lengthy induction time, during which the inhibitor is consumed. After that time, the reaction autoaccelerates gradually and attains the maximum reaction rate at relative conversions of around 80%. This gradual autoacceleration is consistent with the production of free radicals according to the decomposition constant of the initiator and the known Trommsdorf and Norrish–Smith effects that inhibit

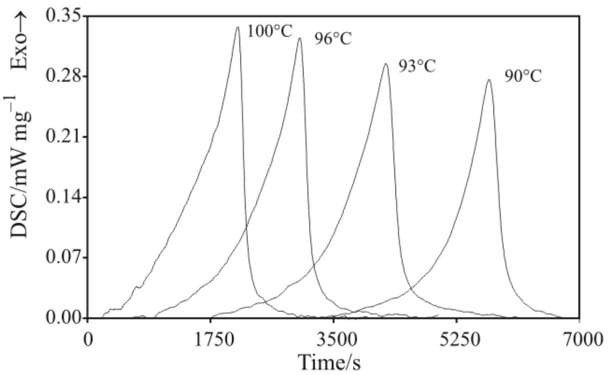

Fig. 1 Isothermal DSC curves at different temperatures for thermal curing

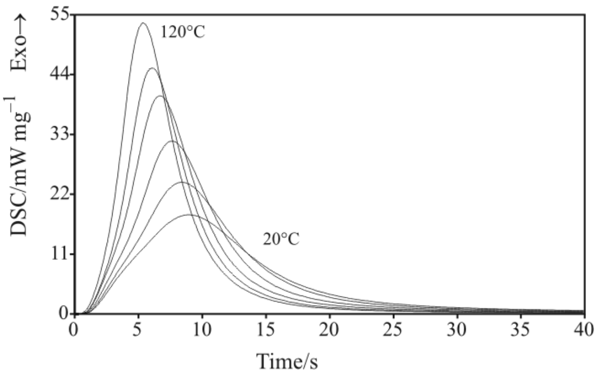

Fig. 2 Isothermal DSC curves at different temperatures (20, 40, 60, 80, 100, 120°C) for photocuring

the terminations [31]. There is no induction time in photocuring since the production of free radicals is almost instantaneous, as is the consumption of the inhibitor. In the latter case, autoacceleration is very pronounced and rapid, and takes place up to relative conversions of around 30%. In both systems, the drop in the reaction rate must be related to the viscosity of the medium, the depletion of reactive species and proximity to vitrification.

Another effect that has been noted is that photocuring gives rise to higher conversions than thermal curing. For example, at a temperature of 100°C, thermal curing produces an ultimate degree of conversion of 79%, while UV radiation produces an ultimate degree of conversion of 88%. One possible explanation is that the UV process is so fast that the system does not occupy its equilibrium volume, as a result of which a surplus free volume remains that allows conversion to attain a level above that allowed by vitrification [10].

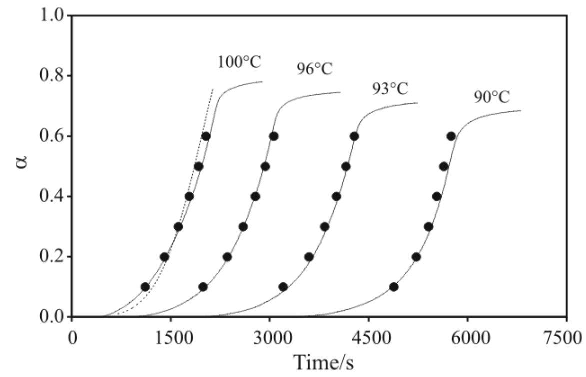

Fig. 3 Experimental and simulated conversion *vs*. time at different temperatures for thermal curing. The continuous line represents the experimental data. The symbols represent the simulated conversions using the isoconversional integral method (Eq. (4)). The discontinuous line represents the simulated conversion using the kinetic triplet at 100°C (E=163.2 kJ mol^{-1}, ln$A$=37.58 s^{-1}, $f(\alpha)=\alpha^{0.25}(1-\alpha)^{0.75}$)

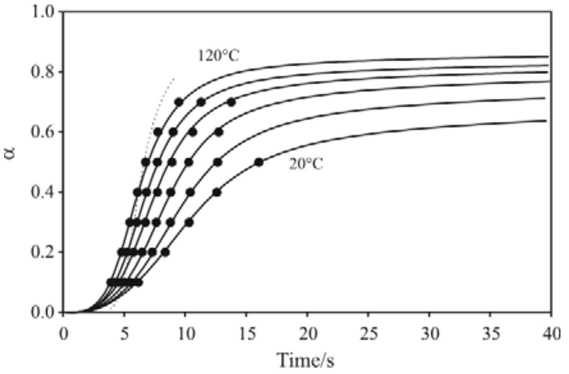

Fig. 4 Experimental and simulated conversion *vs*. time at different temperatures (20, 40, 60, 80, 100, 120°C) for photocuring. The continuous line represents the experimental data. The symbols represent the simulated conversions using the isoconversional integral method (Eq. (4)). The discontinuous line represents the simulated conversion using the kinetic triplet at 120°C (E=7.2 kJ mol^{-1}, ln$A$=2.7 s^{-1}, $f(\alpha)=\alpha^{0.9}(1-\alpha)^{2.1}$)

Figures 3 and 4 show the conversion–time curves, α–t, for the types of curing studied. On the basis of the data of the α–t curves, we determined the integral isoconversional kinetic parameters using Eq. (4). These parameters are shown in Tables 1 and 2. The reliability of the results is seen in the regression coefficients obtained and in the simulation of the α–t curves on the basis of the isoconversional parameters E and ln[$g(\alpha)/A$]. It can be observed that the activation energy is much lower in the case of photocuring than in the case of thermal curing. This result, along with the magnitude of E, is consistent with the results found in the literature [10, 23] and with the initiation mechanisms discussed for the two systems studied. It can also be seen that the variation in E shows an apparent reverse trend as the degree of conversion increases.

Due to the compensation effect between E and ln$A$, we must know the kinetic model and the rate constant in order to discuss the kinetics properly [20, 32, 33]. Although the kinetic parameters vary slightly in the course of curing, the master curves method was used to determine the kinetic model that provides the best

Table 1 Isoconversional kinetic parameters of isothermal thermal curing obtained by DSC

α	E^a/kJ mol^{-1}	ln[$g(\alpha)/A$]^a/s	lnA^b/s^{-1}	r^2	$k_{100°C}{}^c$/s^{-1}	$f(\alpha)$
0.1	166.7	–50.83	47.53	0.9979	0.00196	0.17
0.2	147.9	–44.51	41.39	0.9986	0.00184	0.28
0.3	136.3	–40.64	37.62	0.9989	0.00178	0.37
0.4	127.7	–37.78	34.83	0.9988	0.00174	0.44
0.5	121.3	–35.64	32.76	0.9986	0.00172	0.50
0.6	117.1	–34.21	31.39	0.9982	0.00172	0.54

[a] ln[$g(\alpha)/A$] and E were calculated on the basis of isothermal experiments by DSC, as the intercept and the slope of the isoconversional relationship $\ln t=\ln[g(\alpha)/A]+E/RT$; [b] ln$A$ was calculated using the kinetic model n=0.25, m=0.75 and ln[$g(\alpha)/A$]; [c] Values of the rate constant at 100°C calculated using the Arrhenius equation $\ln k=\ln A-E/RT$

Table 2 Isoconversional kinetic parameters for isothermal photocuring obtained by DSC

α	E^a/kJ mol^{-1}	ln[$g(\alpha)/A$]^a/s	lnA^b/s^{-1}	r^2	$k_{100°C}{}^c$/s^{-1}	$f(\alpha)$
0.1	4.4	–4.08	2.08	0.9896	1.9271	0.10
0.2	5.4	–4.18	2.27	0.9951	1.7034	0.15
0.3	6.1	–4.26	2.43	0.9980	1.5833	0.16
0.4	6.9	–4.39	2.61	0.9977	1.4940	0.15
0.5	8.0	–4.65	2.94	0.9919	1.4156	0.13
0.6	9.0	–4.80	3.18	0.9867	1.3154	0.09
0.7	10.8	–5.14	3.62	0.9805	1.1670	0.06

[a] ln[$g(\alpha)/A$] and E were calculated on the basis of isothermal experiments by DSC, as the intercept and the slope of the isoconversional relationship $\ln t=\ln[g(\alpha)/A]+E/RT$; [b] ln$A$ was calculated using the kinetic model n=2,1 m=0.9 and ln[$g(\alpha)/A$]; [c] Values of the rate constant at 100°C calculated using the Arrhenius equation $\ln k=\ln A-E/RT$

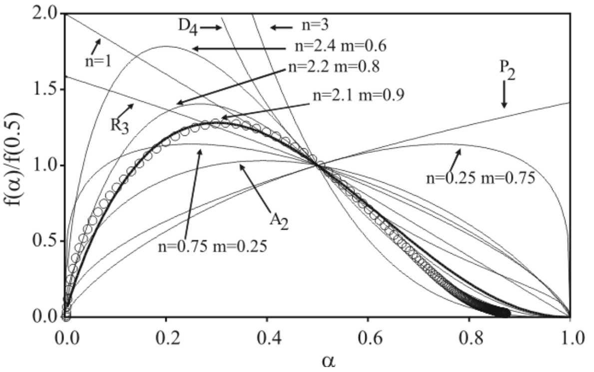

Fig. 5 A comparison of the theoretical differential master plots of $f(\alpha)/f(0.5)$ *vs.* α with the experimental master curve. The symbols correspond to experimental data determined using Eq. (6) for the photocured system

overall description of curing. Figure 5 shows, by way of example, the differential master curves (Eq. (6)) for photocuring. As expected, the model with the best fit over a wide range of conversions is the autocatalytic model, in which n=2.1 and m=0.9. This result is consistent with the maximum observed in the rate of curing and with the conversion at which this maximum occurs. The same kinetic model is obtained by using the integral method. By applying the same methodology to thermal curing, we find that the model with the best fit is the autocatalytic model, in which n=0.25 and m=0.75.

With the system using thermal initiation, it was observed that the activation energy decreases as the degree of conversion increases (Table 1). This effect, which has been observed in the curing of many thermostable systems [23, 34, 35], is apparently related to the autoacceleration of the process. Since the pre-exponential factor also diminishes and this parameter has an effect on the rate constant, which is the inverse of that of E, we cannot assert on the basis of this data that autoacceleration occurs. Table 1 also shows that there is only a slight variation in the value of $k_{100°C}$ and that it even diminishes in the course of curing. The experimental autoacceleration (Fig. 1) observed is therefore not manifest in the rate constant, but rather in the autocatalytic model selected, which makes the reaction rate increase until it reaches its maximum value.

In photocuring, it can be seen that E increases as the degree of conversion increases (Table 2). This effect, already noted by other authors [14], would seem to contradict the autoacceleration observed (Fig. 2). If we note the value of $k_{100°C}$, it can be seen that it decreases in the course of curing. It likewise fails to express the existing autoacceleration, despite the fact that the increase in E is partly compensated by an increase in ln$A$. As in the thermoinduced system, autoacceleration is observed in the differential function $f(\alpha)$. This function increases up to a conversion of 0.3, which is the point to which autoacceleration has been detected experimentally, and subsequently diminishes. The deceleration of the process is observed both in the rate constant and in the kinetic model.

Although the activation parameters in the two systems studied vary in the course of curing, we attempted to find a single kinetic triplet that provides a reasonable description of curing. In order to do so, we used the kinetic models determined using the master curves method and we took (E and A) the average values of the parameters determined isoconversionally as common kinetic parameters (Tables 1 and 2). For the thermally initiated system with benzoyl peroxide, we took the triplet: E=136.2 kJ mol^{-1}, ln$A$=37.6 s^{-1} and $f(\alpha)=\alpha^{0.75}(1-\alpha)^{0.25}$, and for the UV-induced system with 2,2-dimethoxy-2-phenylacetophenone: E=7.2 kJ mol^{-1}, ln$A$=2.7 s^{-1}, $f(\alpha)=\alpha^{0.9}(1-\alpha)^{2.1}$.

Figure 3 shows the simulation of the thermal curing at 100°C using the established kinetic triplet. It can be seen that the simulation fairly accurate, although there are certain deviations at high and low conversions. This result is consistent with the experimental isokinetic temperature (T_{iso}) remaining within the experimental temperature range (T_{iso}=97°C). This means that in the vicinity of T_{iso}, curing can be reasonably well described with a single kinetic triplet and that the kinetic changes observed by modifying the degree of conversion are not very significant [32, 35].

Figure 4 shows the simulation of the photocuring at 120°C using the given kinetic triplet. In this case, it can be observed that the simulation is only correct in the region in which E is similar to that of the triplet. At relatively high conversions, there is substantial deviation, although it falls within the curing region. In this case, the T_{iso} of 212°C is very distant from the experimental temperature range, meaning that a single kinetic triplet does not accurately describe the whole of the curing.

Table 3 sets out some of the kinetic results obtained in the study of photocuring by means of a mechanistic-type methodology. The ratio $k_p/k_t^{1/2}$ was obtained directly from the calorimetric curve, as expressed in Eq. (11). The ratio k_t/k_p was obtained on the basis of the DSC curves corresponding to the dark reaction in samples that were partially cured isothermally with UV radiation, expressed according to Eqs (12) or (13). Figure 6 shows the $(1-\alpha)/(\mathrm{d}\alpha/\mathrm{d}t)$ curves for the dark reactions over time. On the basis of the slope of the linear regression of these latter curves, in the time interval between 9 and 23 s, we obtained the ratio k_t/k_p. We chose this linear interval because the changes in the concentration of the monomer (conversion) in this region are small, as assumed in Eq. (13), but have a residual curing rate that is nevertheless appreciable. Shorter curing times were not used due to the uncertainty of the response time and a substantial variation in conversion [14]. Nor were longer times used, since curing approaches vitrification. Figure 6 also shows the degree of conversion over time for a sample that had attained a conversion of 0.152 prior to the commencement of the dark step. It can be seen that at the start of the dark step, conversion increases notably but after 23 s it increases slowly due to the vitrification process.

Table 3 shows how the global constant k and the ratio $k_p/k_t^{1/2}$ which is proportional to k, increase up to a conversion of 0.4 and then begin to diminish. This result reflects the autoacceleration effect of the curing. In the curves dα/dt–α in the inset of Fig. 7, it can be seen that autoacceleration only occurs up to a conversion of 0.3. The increase in k between the conversion of 0.3 and 0.4 is offset by the decrease in reactive species, producing the overall result of a drop in the reaction rate.

Table 3 Mechanistic kinetic parameters of isothermal photocuring obtained by DSC at 30°C

α	k_t/k_p	$k_p/k_t^{1/2}$/ (L mol^{-1} s^{-1})$^{1/2}$	k_p/ L mol^{-1} s^{-1}	k_t / L mol^{-1} s^{-1}	k^b/s^{-1}	$(\mathrm{d}\alpha/\mathrm{d}t)_{\text{exp}}$/ s^{-1}	$(\mathrm{d}\alpha/\mathrm{d}t)_{\text{calc}}{}^a$/ s^{-1}	E^c/ kJ mol^{-1}	lnA^c/s^{-1}
0.031	58.0	1.0050	58.6	3400	0.0264	0.0248	0.0256	5.9	–1.30
0.049	42.8	1.2050	62.1	2656	0.0317	0.0312	0.0301	7.6	–0.43
0.074	29.2	1.5705	71.9	2096	0.0413	0.0378	0.0382	9.4	0.55
0.107	23.5	2.0396	97.9	2304	0.0536	0.0474	0.0479	8.7	0.54
0.152	22.3	2.5877	149.1	3320	0.0680	0.0573	0.0577	9.9	1.25
0.255	21.0	3.4643	252.3	5304	0.0911	0.0686	0.0679	13.2	2.85
0.410	20.9	3.7397	291.6	6080	0.0983	0.0584	0.0580	13.4	3.01
0.432	20.3	3.6803	274.4	5559	0.0968	0.0547	0.0550	14.1	3.43
0.454	19.9	3.5493	250.7	4989	0.0933	0.0519	0.0510	13.6	3.15

[a]The rate of reaction was calculated using the rate constants and the relationship $\mathrm{d}\alpha/\mathrm{d}t=k_p(\Phi I_{\text{abs}}/k_t)^{1/2}(1-\alpha)$; [b]The global k was calculated using the rate constants and the relationships $\ln k=\ln[k_p(\Phi I_{\text{abs}}/k_t)^{1/2}]$; [c]The global E and ln$A$ were calculated using the rate constant determined at different temperatures and the relationships; $E=E_p-E_t/2$ and $\ln A=\ln[A_p(\Phi I_{\text{abs}}/A_t)^{1/2}]$

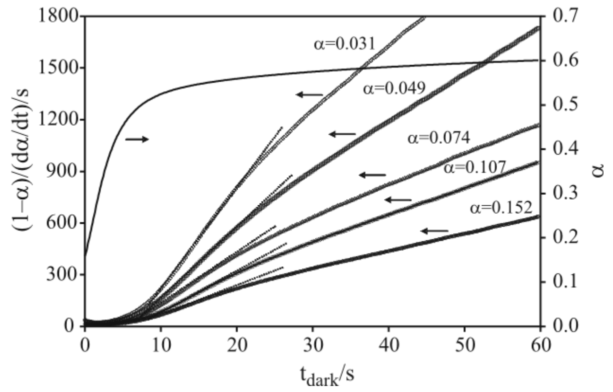

Fig. 6 The symbols show the dependence of (1–α)/(dα/d*t*) *vs.* time at 40°C for the dark reaction of partially photocured material with a conversion before dark reaction, as shown in the figure. The dotted lines provide the slope of the representation over the interval studied. The solid line represents conversion *vs.* time for the dark step with a sample that had attained conversion of 0.152 prior to the commencement of the dark step

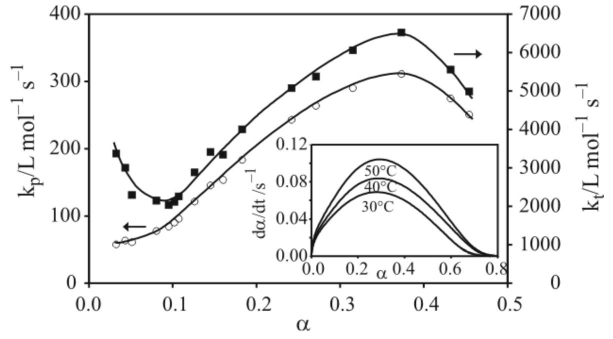

Fig. 7 k_p and k_t *vs*. conversion for samples photocured at 30°C. Inset: dα/d*t* *vs*. conversion at different photocuring temperatures

Most papers note a drop in the constants of termination and propagation until the maximum rate is attained. These papers conclude that during autoacceleration k_t decreases more than k_p, with the resulting increase in the reaction rate [12, 16, 36]. It is generally accepted [37, 38] that termination is controlled by the diffusion of the polymer, while propagation is controlled by the mobility of the units of the monomer. While the polymer chains remain mobile, the (segmental/translational) diffusion of these chains controls the terminations. When this is not the case and only free radical monomers can diffuse and react with the polymer macroradicals, the termination reactions become controlled by the propagation process. At this point there is a substantial decrease in k_t that gives rise to the surge in the reaction rate (autoacceleration). When the decrease in k_t becomes more gradual, along with the decrease in the concentration of reactive species and/or the reduction of k_p, the rate, after attaining a maximum value, tends to drop off until the material is vitrified.

In our work, the rate constants show a trend that is rather different from the one set out above. As an example, Fig. 7, shows the rate constants at a temperature of 30°C, in which three separate regions can be observed. In the first, k_t decreases in conversions of up to 0.1, while k_p increases slightly. At this stage, we can assume that the diffusion of macroradicals starts to be limited and this is where maximum autoacceleration occurs (inset Fig. 7). During the second stage, both k_t and k_p increase greatly and do so in similar proportions. Since the reaction rate is inversely proportional to an exponent 1/2 of k_t, while it depends directly on k_p (Eq. (8)), these similar increases give rise to an acceleration of the reaction rate. At conversions of over 0.4, both constants tend to diminish at a similar rate. This effect, along with the depletion of reactive species and increased viscosity, leads to a deceleration of the curing. The anomalous effect of the increase in the constants during the intermediate stage can be interpreted as an effect of autocatalysis, due to the rise in temperature inside the sample, which accelerates the reaction. The low thermal conductivity of these materials favours the slow dissipation of the heat released by the reaction, which accelerates the curing. This effect has also been observed by other authors in both free radical and cationic photocuring [39, 40].

The similarity between the rate of curing observed experimentally and the rate calculated on the basis of the experimental propagation and termination constants (Table 3) supports the reliability of the parameters obtained.

The apparently contradictory increase in *E* during autoacceleration (Table 3) can, once again, be explained by the compensation effect between *E* and ln*A*. When the global reaction constant *k* is analysed, which includes the value of *E* and ln*A*, an increase during autoacceleration is observed.

In the final section of this paper, we compare the phenomenological and classical mechanistic methodologies with photocuring over the same range of conversions. In order to do so, we performed the isoconversional analysis using the Friedman equation (Eq. (5)), since it is equivalent to the mechanistic Eq. (9) when a 1^{st}-order model is taken.

Table 4 shows the result of the isoconversional analysis. In general, the results are similar to, although not exactly the same as, those obtained by means of integral isoconversional analysis (Table 2) if the same kinetic model is taken (n=2.1, m=0.9). The reliability of the results is highlighted by the regression coefficients and by the similarity between the experimental reaction rate and the rate calculated on the basis of the isconversional data. *E* and ln*A* increase as the degree of conversion rises, but since these parameters compensate each other, the rate

Table 4 Phenomenological kinetic parameters at 30°C for isothermal photocuring obtained by DSC

α	E^a/ kJ mol^{-1}	$\ln[f(\alpha)A]^a$/ s^{-1}	r^2	$(d\alpha/dt)_{exp}$/ s^{-1}	$(d\alpha/dt)_{calc}{}^b$/ s^{-1}	$f(\alpha)=\alpha^{0.9}(1-\alpha)^{2.1}$ (autocatalytic)		$f(\alpha)=(1-\alpha)$ n^{th} order with n=1	
						$\ln A^c$/s^{-1}	k^d/s^{-1}	$\ln A^c$/s^{-1}	k^d/s^{-1}
0.031	7.7	–0.64	0.9897	0.0248	0.0250	2.56	0.6088	–0.64	0.0258
0.049	8.0	–0.30	0.9838	0.0312	0.0315	2.52	0.5291	–0.30	0.0331
0.074	9.4	0.48	0.9805	0.0378	0.0384	2.99	0.4685	0.48	0.0415
0.107	9.5	0.72	0.9874	0.0474	0.0479	2.97	0.4541	0.72	0.0537
0.152	10.6	1.36	0.9998	0.0573	0.0575	3.40	0.4429	1.36	0.0678
0.255	12.4	2.24	0.9907	0.0686	0.0695	4.09	0.4410	2.24	0.0933
0.410	14.5	2.91	0.9871	0.0584	0.0595	4.83	0.4018	2.91	0.1008
0.432	14.8	2.97	0.9822	0.0547	0.0557	4.91	0.3889	2.97	0.0981
0.454	14.2	2.71	0.9803	0.0519	0.0530	4.69	0.3846	2.71	0.0971

[a] $\ln[f(\alpha)A]$ and E were calculated on the basis of isothermal experiments by DSC, as the intercept and the slope of the isoconversional relationship $\ln(d\alpha/dt)=\ln[f(\alpha)A]-E/RT$; [b] The values of the rate of reaction at 30°C calculated using isoconversional kinetic parameters and Eq. (3); [c] $\ln A$ was calculated using the kinetic model n=2.1, m=0.9 or n=1 and $\ln[f(\alpha)A]$; [d] The values of the rate constant at 30°C were calculated using the Arrhenius equation $\ln k=\ln A-E/RT$

constants diminish slightly and the increase in the reaction rate is associated with the chosen autocatalytic model. This result is significantly different for the result obtained mechanistically and only the activation energies obtained through both procedures are similar (Tables 3 and 4). This is logical, given that E is independent of the chosen model.

In order to compare the two methodologies in greater depth, we imposed a 1st-order model on the phenomenological procedure, even though this is not the model that describes the curing phenomenologically. Table 4 shows the results obtained. It can be seen that the phenomenological results are now similar to the mechanistic results. The values for $\ln A$ are of the same order of magnitude and the global reaction constants k are practically identical.

On the basis of the comparison of the two methodologies, we can conclude that both the phenomenological procedure and the mechanistic procedure can be used to describe and simulate curing correctly. Using the mechanistic methodology, the autocatalytic effect is denoted by an increase in the rate constant, while the kinetic model is decremental. However, using the phenomenological methodology, the value of the rate constant is not very significant (it diminishes slightly) and the increase in the reaction rate is seen in the autocatalytic kinetic model. The results of our work do not allow us to discern which of the two procedures is more accurate, since different hypotheses are used in each of them.

The most questionable aspects of the phenomenological methodology include the possible interpretation of the kinetic models, which in some cases are merely descriptions of a rate curve, with no physical–chemical interpretation, and the assumption of a single constant model throughout the curing process. If we only use isoconversional methods, these problems can be resolved. In this case, fewer hypotheses are made, the methodology is simple, and it can be applied to a wide range of conversions. The only drawback with this approach is that the pre-exponential factor and the kinetic model are grouped into a single parameter.

The mechanistic methodology is, a priori, more attractive, since it allows us to obtain all the kinetic parameters involved in the process (k_p, k_t, k, E, A, etc.), but it does have certain drawbacks. The main drawbacks are that the application of this methodology is costly, since it combines steady-state testing with light and non-steady-state testing without light, and that it is only possible to obtain parameters within a given range of conversions. The numerous hypotheses that must be made using this methodology, and which are not required with the isoconversional methodology, can also give rise to doubts in connection with the interpretation of some of the mechanistic kinetic parameters.

Conclusions

In phenomenological terms, the curing of dimethacrylate monomers that is induced thermally or by UV radiation is of the autoaccelerating type, although photocuring occurs at much higher reaction rates. In thermal curing, the activation energy is high and is strongly influenced by the decomposition of the initiator. Conversely, in UV-induced curing the activation energy is low, due to the fact that the decomposition of the initiator is an instantaneous process that occurs with an activation energy of nearly zero. A single kinetic triplet was established for both types of photocuring, using isoconversional analysis and the master curves method. For the UV-photocuring, this triplet only describes the curing approximately.

Making use of considerations about the mechanism of the reaction, it was seen that the propagation and termination constants vary with the conversion. The decrease of k_t at the start of curing is related to a limitation on mobility. The increase of k_t and k_p is associated with the heat released in the curing process.

Comparison of the phenomenological and mechanistic methodologies has revealed that both methodologies allow a description of photocuring to be made, although the kinetic results are different. In phenomenological terms, autoacceleration is shown in the kinetic model of the autocatalytic type, while in mechanistic terms this same phenomenon is noted through the rate constant, which increases. In general, the mechanistic approach is more physically and chemically significant, but it is more complex and requires more hypotheses. However, the phenomenological approach is easier to use and requires fewer simplifications, although its physical and chemical interpretation is unclear.

We can describe the curing kinetically, with no need to enter into any considerations as to the reaction mechanism or simplifications, by means of isoconversional analysis. In this case, the description of kinetics is based upon the activation energy and a second parameter that groups the pre-exponential factor with the kinetic model.

Acknowledgements

The authors would like to thank the CYCIT (Comisión Interministerial de Ciencia y Tecnología) and FEDER (European Regional Development Fund) (MAT2004-04165-C02-02).

References

1 J. Jancar, W. Wang and A. T. Dibenedetto, J. Mater. Sci. Mat. Med., 11 (2000) 675.
2 S. H. Dickens, J. W. Stansbury, K. M. Choi and J. E. Floyd, Macromolecules, 36 (2003) 6043.
3 P. Burtscher, Dent. Mater., 9 (1993) 218.
4 G. P. Simon, P. E. M. Allen, D. J. Bennett, D. R. G. Williams and E. H. Williams, Macromomecules, 22 (1989) 3555.
5 S. P. Pappas, Ed., Radiation Curing: Science and Technology, Plenum Press, New York 1992.
6 J. P. Fouassier and J. F. Rabek, Eds, Radiation Curing in Polymer Science and Technology, Elsevier Applied Science, London 1993.
7 E. Andrzejewska, L.-A. Lindén and J. F. Rabek, Polym. Int., 42 (1997) 179.
8 E. Andrzejewska, Polymer, 37 (1996) 1039.
9 V. Müller, S. Jockusch and H.-J. Timpe, J. Polym. Sci. A, Polym. Chem., 30 (1992) 1755.
10 L. Lecamp, B. Youssef, C. Bunel and P. Labaudy, Polymer, 38 (1997) 6089.
11 C.-W. Huang, Y.-M. Sun and W.-F. Huang, J. Polym. Sci. A, Polym. Chem., 35 (1997) 1873.
12 L. Lecamp, B. Youssef, C. Bunel and P. Labaudy, Polymer, 40 (1999) 1403.
13 E. Andrzejewska, Polymer, 37 (1996) 1047.
14 G. R. Tryson and A. R. Shultz, J. Polym. Sci. Polym. Phys. Ed., 17 (1979) 2059.
15 W. Z. Xia and W. D. Cook, Polymer, 44 (2003) 79.
16 J. L Mateo, J. Serrano and P. Bosch, Macromolecules, 30 (1997) 1285.
17 D. C. Watts, Dent. Mater., 21 (2005) 27.
18 P. J. Flory, Principles of Polymer Chemistry, Cornell University Press: Ithaca, New York 1953.
19 W. D. Cook, Polymer, 33 (1992) 2153.
20 A. Cadenato, J. M. Morancho, X. Fernández-Francos, J. M. Salla and X. Ramis, J. Therm. Anal. Cal., 89 (2007) 233.
21 F. J. Gotor, J. M. Criado, J. Málek and N. Koga, J. Phys. Chem., A 104 (2000) 10777.
22 J.-D. Cho, H. T. Ju and J.-W. Hong. J. Polym. Sci. A, Polym. Chem., 43 (2005) 658.
23 J. M. Salla and X. Ramis, Polym. Eng. Sci., 36 (1996) 835.
24 S. Vyazovkin and N. Sbirrazzuoli, Macromol. Rapid Commun., 21 (2000) 85.
25 S. Vyazovkin and C. A. Wight, Ann. Rev. Phys. Chem., 48 (1997) 125.
26 H. Friedman, J. Polym. Sci., C6 (1964) 183.
27 N. Sbirrazzuoli, Y. Girault and L. Elégant, Thermochim. Acta, 293 (1997) 25.
28 J. M. Criado, L. A. Pérez-Maqueda, F. J. Gotor, J. Málek and N. Koga, J. Therm. Anal. Cal., 72 (2003) 901.
29 T. Ozawa, Bull. Chem. Soc. Jpn., 38 (1965) 1881.
30 A. R. Shultz, J. Polym. Sci. Part C, 25 (1968) 115.
31 G. Odian, Principles of Polymerization, 3rd Ed., Wiley, New York 1991.
32 S. Vyazovkin and W. Linert, Chem. Phys., 193 (1995) 109.
33 S. J. García, X. Ramis, A. Serra and J. Suay, J. Therm. Anal. Cal., 83 (2006) 429.
34 J. M. Salla, A. Cadenato, X. Ramis and J. M. Morancho, J. Therm. Anal. Cal., 56 (1999) 771.
35 S. Vyazovkin, Int. Rev. Phys. Chem., 19 (2000) 45.
36 K. S. Anseth, C. M. Wang and C. N. Bowman, Polymer, 35 (1994) 3243.
37 T. F. Scott, W. D. Cook and J. S. Forsythe, Polymer, 44 (2003) 671.
38 S. K. Soh and D. C. Sundberg, J. Polym. Sci., Polym. Chem. Ed., 20 (1982) 1315.
39 B. Falk, S. M. Vallinas and J. V. Crivello, J. Polym. Sci. A, Polym. Chem., 41 (2003) 579.
40 C. Decker, Macromol. Rapid Commun., 23 (2002) 1067.

Received: June 12, 2007
Accepted: January 30, 2008

DOI: 10.1007/s10973-007-8432-x